

Effect of Green Light from Doubled Frequency Neodymium-Doped Yttrium Aluminum Garnet (Nd:YAG) Laser in the Nanosecond Range on Rabbit's Lens –In Vitro Study

Salwa Abdelkawi¹, Nahed Hassan², Monazah Khafagi³

¹Department of Vision Sciences, Biophysics and Laser Science Unit, Research Institute of Ophthalmology, Giza, Egypt.

²Department of Biochemistry, Biophysics Lab, National Research Center, Cairo, Egypt.

³Department of Spectroscopy, Physics Division, National Research Center, Cairo, Egypt.

Abstract:

Introduction: The unprotected eye is extremely sensitive to laser radiation and can be permanently damaged from direct or reflected beams. The area of the eye damaged by laser energy is dependent upon the wavelength of the incident laser beam, duration of exposure and tissue characteristics. This study aims to investigate the effect of intense green light from doubled frequency Neodymium-Doped Yttrium Aluminum Garnet (Nd:YAG) (532 nm) in the nanosecond range on the protein of rabbits lenses after short and prolonged (6, 18 seconds) exposures.

Methods: The fundamental wavelength (1064 nm) was frequency doubled in β - Barium Borate (BBO) crystal for second harmonic generation (SHG). Rabbits' lenses were irradiated in vitro, and the effect of the laser was evaluated by comparing the protein concentration, structure and conformation by sodium dodecyl sulphate polyacrylamide electrophoresis (SDS-PAGE) and Fourier transform infrared spectroscopy (FTIR).

Results: The results indicated a significant change in the soluble protein content, the molecular weights and the backbone structure of different lens crystallin fractions. These effects were more distinct when using laser with prolonged irradiation for 18 seconds than for 6 seconds.

Conclusion: Irradiation with frequency doubled Nd-YAG green laser seem to be cataractous if the lens is exposed to laser that is intense enough to warrant thermal protein aggregation, folding and denaturation.

Keywords: green light; Nd:YAG; SDS-PAGE

Please cite this article as follows:

Abdelkawi S, Hassan N, Khafagi M. Effect of Green Light from Doubled Frequency Nd:YAG Laser in the Nanosecond Range on Rabbit's Lens –In Vitro Study. *J Lasers Med Sci* 2012; 3(4):165-74

***Corresponding Author:** Salwa Abdelkawi, Department of Vision Sciences, Biophysics and Laser Science Unit, Research Institute of Ophthalmology, 2 El-ahram St. Giza, Egypt. Postal code: 12511; Fax: +202 35735688; Phone: +20100 1670590; E-mail: saelkawi@yahoo.com

Introduction

The use of laser technology particularly for the eye has the potential to revolutionize the way used to deliver and receive health care. Some of the technologies currently in trials will benefit from

advances in new laser delivery systems. However, this is not without possible risks and disadvantages- as with any technology, there may be unanticipated side effects and complications. One of the most commonly used technologies is frequency doubling or second-harmonic generation (SHG). SHG is a nonlinear optical

process carried out by placing a nonlinear medium in a laser beam. Therefore, photons interacting with a nonlinear material are effectively combined to create new photons with twice the energy, twice the frequency and half the wavelength of the initial photons, which created the required high intensity monochromatic light (1,2).

While there are many types of nonlinear media, the most common media are crystals. Commonly used crystals are BBO (β -barium borate); KDP (potassium dihydrogen phosphate); KTP (potassium titanyl phosphate); and lithium niobate (3). These crystals have the necessary properties of being strongly birefringent (necessary to achieve phase matching) and having specific crystal symmetry. These crystals are transparent for both the impinging laser light and the frequency-doubled wavelength. In addition, they have high damage thresholds, which make them resistant against the high-intensity laser light. BBO is an efficient crystal for the intracavity SHG of high power Neodymium-Doped Yttrium Aluminum Garnet (Nd:YAG) lasers. Because of a small acceptance angle and large walk-off, good laser beam quality (small divergence, good mode condition, etc.) is the key for BBO to obtain high conversion efficiency (1,3).

In biological and medical science, SHG microscopy has been used for extensive studies of the cornea and lamina cribrosa sclerae (4,5). SHG is also used in laser industry to develop green 532 nm lasers from 1064 nm. Moreover, in high quality diode lasers, the crystal is coated on the output side with an infrared filter to prevent leakage of intense infrared light (1064 nm) into the beam. This wavelength is invisible, and do not trigger the defensive blink-reflex reaction in the eye, therefore, can be a special hazard to the human eyes. Nevertheless, some green laser pointer products have become available on the market, which omit the expensive infrared filter, often without warning (6). In addition, laser prostatectomy has evolved as an advantageous technique for the efficient removal of prostate tissue for the treatment of symptomatic benign prostatic hyperplasia (BPH), with an excellent safety profile (7). The frequency doubled Nd:YAG laser (532 nm) can be used for photochemical bleaching in cases of teeth whitening and presents some advantages over most available bleaching products (8).

Cataract is a major health problem, accounting for nearly 20 millions cases of blindness globally and an even greater number of cases of low vision (9). Cataract is characterized by increased absorption

and scattering of light by the eye lens resulting in a decreased transmission of light to the retina (10,11). Crystallins is a major class of proteins in the eye lens composed of α -crystallin, β -crystallin and γ -crystallin (9,10). Proper supra-molecular assembly of these proteins is critical to maintain lens transparency (11).

In case of cataract, lens crystallin gradually become high molecular weight aggregates and lead to the formation of insoluble protein (12).

Recently, vibrational spectroscopy using Fourier transform infrared spectroscopy (FTIR) has become increasingly important in the study of the molecular structure of various biological samples due to its simple, fast, non-destructive method, powerful and convenient functions (13-15). Moreover, previous studies have evaluated the composition and conformational changes of lens proteins and the calcification of intraocular lens by using FTIR (16,17).

The present study is the first to evaluate the effects of green laser irradiation with doubled frequency Nd:YAG laser source on the structure of rabbits lenses protein using sodium dodecyl sulphate polyacrylamide electrophoresis (SDS-PAGE) and FTIR spectroscopy. This was done in vitro by using BBO crystal for second harmonic generation (SHG) and two different exposure times (6,18 seconds). With this technique, the 1064 nm in the infrared range output from Nd:YAG laser can be converted to green visible light, with wavelengths of 532 nm.

Methods

Biological Material

Lenses of good optical quality were enucleated from 18 mature (3 month's age) New Zealand rabbits obtained from the animal house of the Research Institute of Ophthalmology, Giza, Egypt. All procedures were conducted according to the principles enunciated in the Guide for Care and Use of Laboratory Animals. They were subjected to experimental protocols approved by the local experimental ethics committee of ophthalmic and vision research.

Laser System

Laser irradiation was carried out in the National Research Center, Dokki, Egypt, with Neodymium YAG (Nd:YAG) solid-state laser (Continuum laser, PRLI 8000, Electro-optics, Inc., Wyandotte, MI, USA)

operating at 12 KHz. The long cavity of the laser system yield a full width at half- maximum pulse duration (FWHM) of 7 ns; energy of 2mJ for individual pulse and beam diameter of 10 mm to ensure that the entire area of the lenses was irradiated. The fundamental wavelength (1064 nm) in the infrared range was frequency doubled using β - barium Borate (BBO) crystal for second harmonic generation (SHG) to yield 532nm green light. The lenses were divided into three groups. One group served as control (n=12 eye lenses) and the other two groups (n=12 eye lenses each) were irradiated with a collimated laser beam for 6sec and 18 Sec respectively.

Protein Analysis

Rabbits lenses were weighed, homogenized in bi-distilled water (using cell homogenizer type Tübingen 7400, Germany), and centrifuged at 53,000 g in a bench centrifuge (Awel centrifuge MS 20-R, Blain, France). The resultant supernatant, which contains the soluble lens proteins, was used to determine the total soluble lens proteins of the crystalline (18).

Protein composition of the lens samples was analyzed according to its molecular weight by SDS-PAGE using 3% stacking gel and 10% separating gel (19). The gel was scanned using scanner model SG-700 Imaging Densitometer (Bio Rad).

Fourier Transform Infrared Spectroscopy

The structure and bond formation of the lyophilized soluble lens protein were confirmed by recording FTIR spectra. The FTIR spectra were collected for these samples using Fourier transform infrared spectrometer (FT/IR-6100, Jasco, Japan). All spectra were recorded in the range ($4000-400\text{ cm}^{-1}$), the number of scans was 128, and the resolution was 4 cm^{-1} and scan speed 2 mm/s . Measurements were made with an IR cell using potassium bromide (KBr) technique (20). De-convolution and second-derivative methods have been applied to locate the position of the overlapping components of the amide I and amide II bands and assign them to different secondary structures (21,22).

Statistical Evaluation

The values of protein concentration were expressed as the mean \pm SD (standard deviation) for n=4 independent measurements. Statistical analysis of the

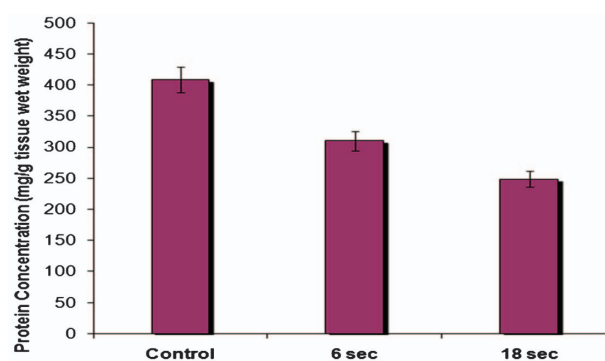


Figure 1. Protein concentration of rabbits' lenses exposed to green light from doubled frequency Nd:YAG laser of 532 nm for 6 and 18 seconds.

data was performed using Students' *t*-test. Statistical significance was assumed at a level of $P < 0.05$ (23).

Results

Lens Protein Concentration

The protein content for the control group was $409 \pm 0.8\text{ mg/gm}$ tissue wet weight (Figure 1). The data indicated that there was a high significant reduction ($P < 0.01$) in the protein content for the group treated for 6 sec with a mean value of $312.7 \pm 2.5\text{ mg/gm}$ tissue wet weight and percentage change of -23.5%. After laser exposure for 18 sec there was a very high significant decrease in protein content ($P < 0.001$) with a percentage change of -38%.

SDS- PAGE Results

The analysis of the control sample was characterized by the presence of nine bands representing different soluble protein fractions with their specific intensities and molecular weights ranging from 196-8 KD (Figure 2). Moreover, in the other groups, the profile of the bands in the high and low molecular weight regions were significantly changed according to the time of exposure to green light from doubled frequency Nd:YAG laser of 532 nm for 6 and 18 seconds respectively. The electrophoresis pattern for the lens of rabbits exposed to green laser for 6 seconds (Figure 2, panel a) showed obvious changes in the mobility and the intensity of the protein fractions compared with the control. The pattern which was shifted towards high molecular weight covered a range from 205 KD to 25 KD accompanied by the increase in the intensity of two fractions at the high molecular weight region (205,107

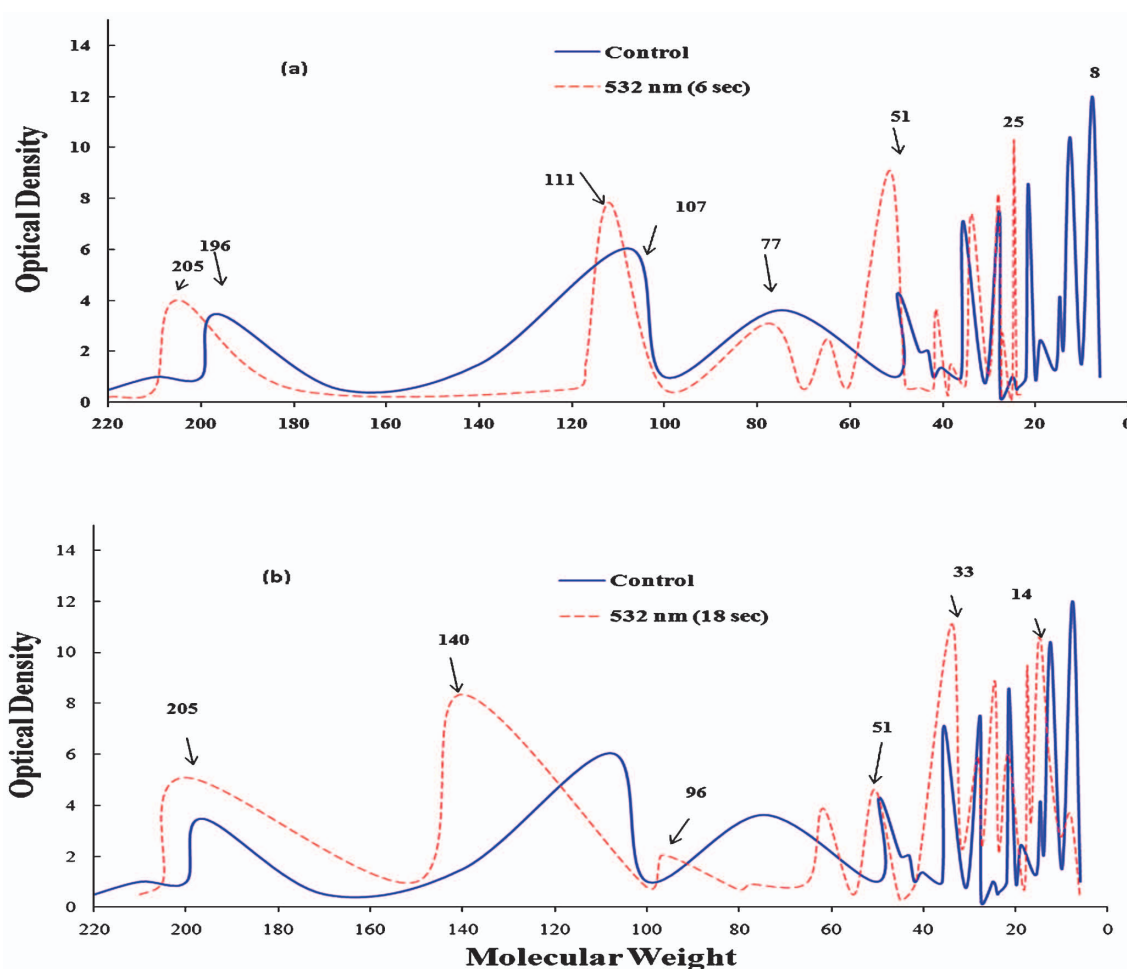


Figure 2. SDS- PAGE of rabbits lenses: panel (a) and panel (b) represents control sample and lenses exposed to green light from doubled frequency Nd:YAG laser of 532 nm for 6 seconds and 18 seconds.

KD), and the maximum peak intensity was noticed at 51KD. On the other hand, the electrophoresis pattern for lens protein exposed to doubled frequency laser for 18 seconds (Figure 2, panel b) revealed broadening, progressive increase in molecular weight at 205 KD, 140 KD and a small shoulder at 96 KD accompanied by an increase in peaks intensity at the high and low molecular weight regions.

FTIR Spectroscopy Results

The FTIR spectrum in NHOH region of control rabbits' lens (Figure 3) (a) revealed the presence of the band at 3435 cm^{-1} corresponds to the $-\text{OH}$ asymmetric, while the bands at 2966 cm^{-1} and 2921 cm^{-1} is attributed to asymmetric C–H stretching vibrations while the band at 2852 cm^{-1} is attributed to symmetric C–H stretching vibrations. Moreover, there were dramatic changes in the spectra of rabbit

lens according to the irradiation time. For 6-seconds irradiation, the changes can be noticed in the OH region at 3435 cm^{-1} and are characterized by reduction in its band intensity. In addition, the intensities of CH bands at 2921 and 2852 cm^{-1} were increased. On the other hand, as the irradiation time was increased to 18 sec, the intensity of OH and C–H bands were greatly reduced, and the band at 2966 cm^{-1} disappeared. Moreover, N–H stretching vibration band at 3007 cm^{-1} can be noticed at lenses irradiated for 6 seconds but disappeared at those irradiated for 18 seconds.

Figure 4 illustrates the FTIR spectra for control rabbit lenses and those irradiated with 532 nm doubled frequency Nd:YAG laser for 6 and 18 seconds in the frequency range $1800 - 800\text{ cm}^{-1}$. For control rabbit lenses, the maximum peaks of amide I bands at 1641 cm^{-1} and the N–H bending vibration were observed at around 1546 cm^{-1} (amide II). The band at 1455 cm^{-1} is assigned to CH₂ bending and at 1401

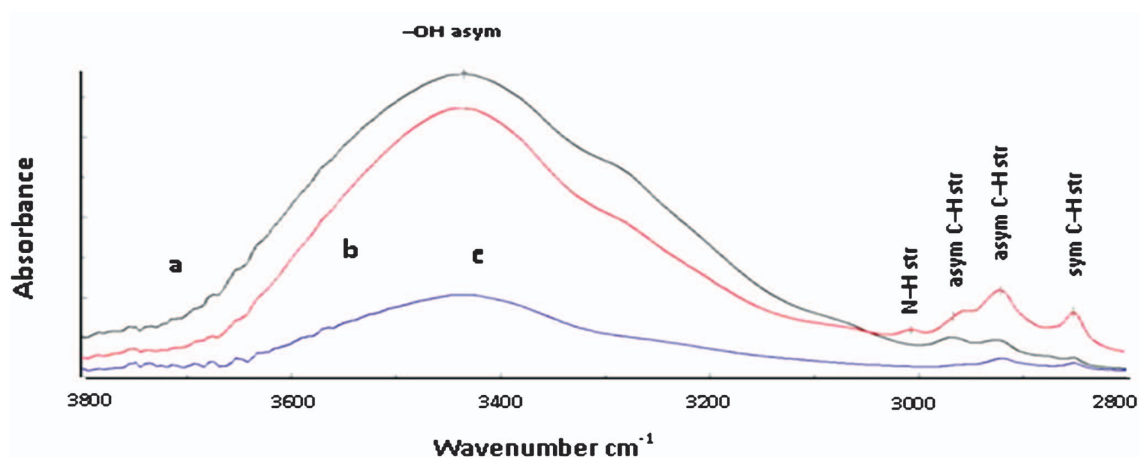


Figure 3. FTIR spectra in NHOH region for (a) control rabbit lenses and lenses exposed to doubled frequency Nd:YAG laser of 532 nm for (b) 6 seconds and (c) 18 seconds (3800–2800 cm^{-1}).

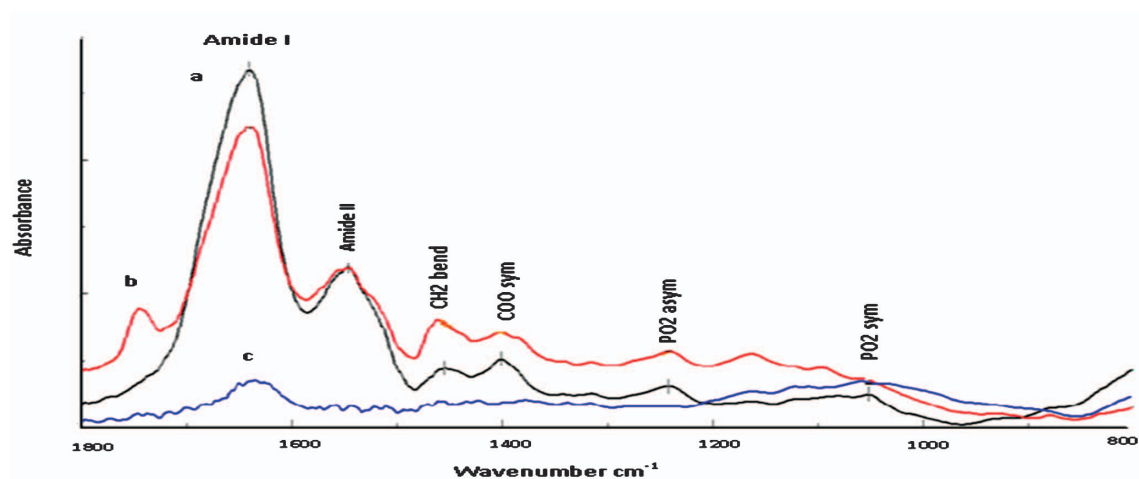


Figure 4. FTIR spectra in the fingerprint region for (a) control rabbit lenses and lenses exposed to doubled frequency Nd:YAG laser of 532 nm for (b) 6 seconds and (c) 18 seconds (1800–900 cm^{-1}).

cm^{-1} was due to symmetric stretching of carboxylate (COO). The bands at 1241cm^{-1} and 1051cm^{-1} were due to the asymmetric and symmetric phosphate stretching modes (PO_2) in the lenses. After exposure to frequency doubled Nd:YAG laser for 6 seconds, the intensity of amide I band decreased. The intensity of peak at 1546cm^{-1} for NH bending (amide II) match the control while that of bands at 1455cm^{-1} (CH_2 bend), 1401cm^{-1} (sym COO str) and 1241cm^{-1} (asym PO_2 str) significantly increased. After exposure to Nd:YAG laser for 18 seconds, the intensity of most peaks was greatly reduced.

The characteristic peak for each component in de-convoluted curve FTIR spectra for control and irradiated lenses was illustrated in Figure 5. In the region from 3800 to 2800cm^{-1} , there were the C–H and N–H stretching vibrations and water bands. The characteristic spectral bands for molecular structure

of control lenses revealed the presence of well defined bands at 3439cm^{-1} and 3287cm^{-1} which are characteristic for asymmetric and symmetric stretching vibration of OH respectively, while the NH group appeared at 3218cm^{-1} . The asymmetric and symmetric CH_2 stretching bands were observed at 2854cm^{-1} and 2926cm^{-1} , while the band at 3079cm^{-1} and 2968cm^{-1} are due to the asymmetric and symmetric $-\text{CH}_3$ stretching mode of the methyl groups. These CH_3 stretching modes might be assigned to both the end-methyl groups of lipids and the methyl groups of the side chains of proteins (24).

The secondary structure IR spectra curve for control and irradiated lenses (Figure 6) revealed that, the control lenses peaks at 1638 , 1394 , 1243 , 1169 , 1111 and 1051cm^{-1} were shifted to 1639 , 1390 , 1242 , 1165 , 1094 and 1036cm^{-1} in the lenses exposed to Nd:YAG Laser for 6 sec. Moreover, the peaks were shifted to

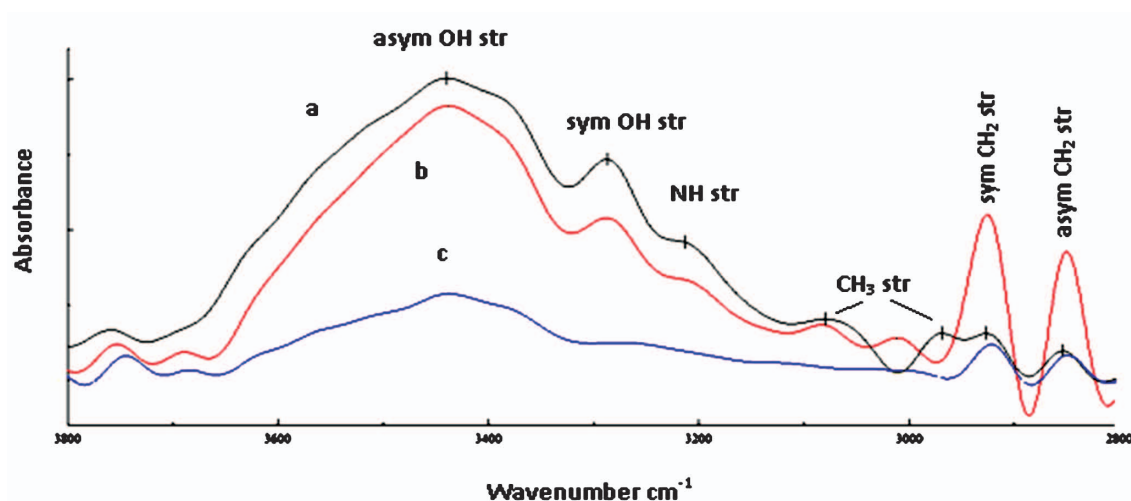


Figure 5. De-convoluted FTIR spectra for wavenumber ranging from 3800–2800 for (a) control rabbit lenses, lenses exposed to doubled frequency Nd:YAG laser of 532 nm for (b) 6 seconds and (c) 18 seconds.

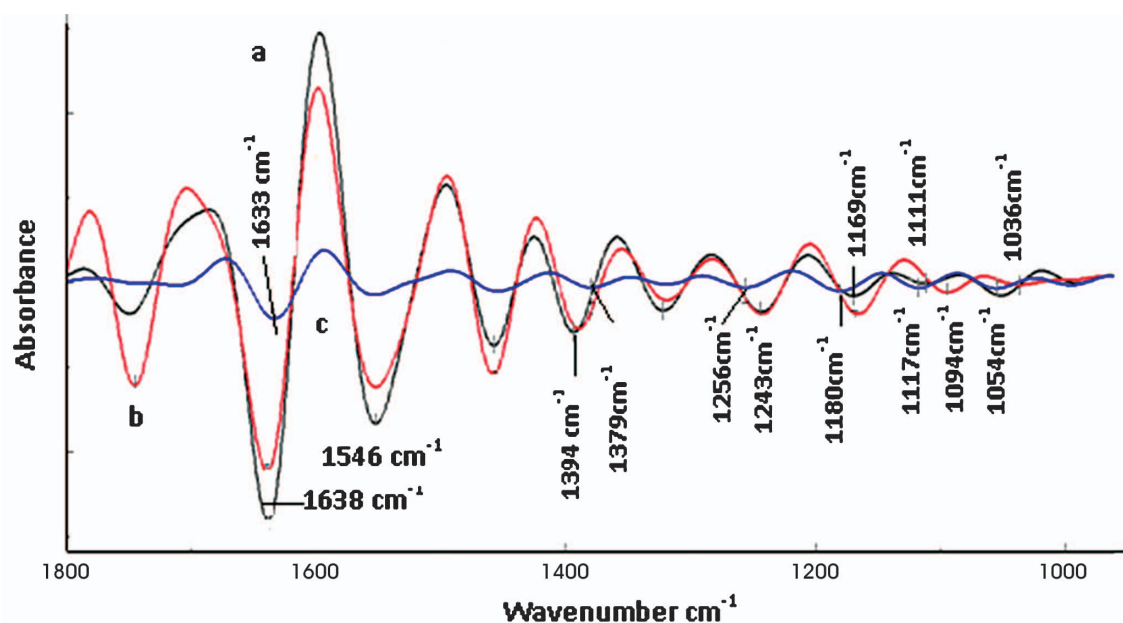


Figure 6. Second-derivative infrared spectra recorded from a solution rabbit lenses from 1800–1000 for (a) control rabbit lenses, lenses exposed to doubled frequency Nd:YAG laser of 532 nm for (b) 6 seconds and (c) 18 seconds.

1633, 1379, 1256, 1180, 1117 and 1054 cm^{-1} in the lenses exposed to doubled frequency Nd:YAG laser for lens exposed to 18 sec. In addition, a marked difference in peak intensity of amide I band for the control lenses and irradiated lenses was observed.

Amide I and amide II bands are always used as an indicator to predict the protein secondary structure because they are sensitive to hydrogen bonding (21,22). The peak intensity ratio of amide I / amide II (1638:1546 cm^{-1}) of control lenses was 1.27, whereas in the spectra of irradiated lenses with 6 seconds this ratio (1639:1546 cm^{-1}) was 1.33, but was 1.75

for irradiated lenses with 18 sec in the intensity ratio of 1633:1546 cm^{-1} .

Discussion

The optically transparent refractive layers of the eye, such as the cornea and lens, do not absorb electromagnetic radiation in the visible or near-infrared spectrum at low power densities, allowing light to pass through without alteration of these tissues. At higher power densities, these structures do absorb the light energy, leading to plasma generation and tissue

disruption (25). The first practical use of near-infrared lasers in clinical ophthalmology was the Nd:YAG laser (1064 nm). Nd:YAG was widely used for opening of opacified posterior lens capsules after cataract surgery, iridotomy in pupillary-block glaucoma, and in lyses of vitreous membranes. The Nd:YAG laser has pulse duration in the nanosecond (10^{-9} second) range and produces photo-disruption at its focal point in tissue, resulting in a rapidly expanding cloud of free electrons and ionized molecules "plasma", in turn creating an acoustic shock wave that disrupts the treated tissue (26). Nd:YAG laser causes functional changes to the lens crystallin results in the development of protein aggregates with the formation of opacity and eventually formation of cataract (27). Moreover, this large volume of collateral damage renders this laser impractical for use in corneal surgery and iridotomy, which demands much higher precision (28). Frequency doubling or SHG is a technique used to produce a wavelength that is one-half of the fundamental wavelengths of a laser. For the 1064nm fundamental wavelength of Nd:YAG, the second harmonic generation is 532 nm. There are several reasons to consider the use of a doubled frequency laser: the shorter wavelength will be absorbed more efficiently with some target materials, and the shorter wavelength has the potential to produce a beam focus spot, which is 50% smaller than that produced by the fundamental wavelength. Therefore, in the present work the effect of intense green light obtained from frequency doubling of Nd:YAG laser in the nanosecond range (7×10^{-9} second) on lens was documented by measuring protein concentration, composition and conformational change using SDS- polyacrylamide gel electrophoresis and FTIR spectroscopy after short and prolonged exposure for 6 and 18 seconds respectively.

The present data indicated a decrease in soluble protein concentration due to exposure to doubled frequency Nd:YAG laser and this decrease is a sign for increased non-soluble proteins. The structural changes in the lens crystallin are also evidenced by SDS-PAGE. It was clear from the scanning curves that, lens crystallin fractions of the treated groups exhibited a different behavior from control. There were changes in the high and low molecular weight regions, electrophoresis mobility and intensity of different peaks representing different crystallin fractions. These results allow some valid conclusions to be drawn about the mechanisms, which induce cataract formation after irradiation with SHG, doubled frequency, short

wavelengths. One of the mechanisms proposed to explain lens opacification is the oxidation of crystallin by reactive oxygen species (ROS) generated from the interaction between laser and water molecules. The overproduction of ROS upon exposure to laser, results in oxidative stress and imbalance between the pro-oxidants and antioxidant. Once this imbalance takes place, cellular molecules may be damaged by the predominant free radicals. This leads to oxidative modification of the cellular molecules. In this respect, the photochemical or photo-damage formed upon exposure of lens protein to laser irradiation because of its high pulse energy may leads to the formation of cross-linked proteins and the development of cataracts (29). Based on these mechanisms, it seems likely that, these changes are dependent on the wavelength and exposure time, and thus the lesions are likely to be thermal, induced by absorption and dissipation of heat in the lens tissues (30).

It is well known that, lens proteins are prone to aggregation by heating and lens transparency is intimately related to the three-dimensional arrangement of the lens proteins (31-33). Such changes may be due to oxidation of lens protein by Nd:YAG laser, giving rise to disulphide bond formation, and induce cross-linking. Therefore, enhancing protein aggregation resulting in protein modifications is indicative of oxidative damage. Photo-oxidation was believed to play a role for cataract genesis and was most likely involved in protein conformational changes that are observed in lens protein upon exposure to laser irradiation. This process leads to protein denaturation, aggregation and cataract formation (34-35).

Recently, vibration spectroscopic FTIR is a valuable technique due to its high sensitivity in detecting changes in the molecular constituents of tissues (13,36,37). Proteins carry out most of the important tasks in living cells. They must fold to their proper, unique three-dimensional structure to perform these important tasks. Poor protein folding and insolubility lead to inefficient functional protein (38).

The amide I band of the originally infrared spectra, in general, is too complex and featureless to be of quantitative significance, and it is a superposition of several structural components. The amide I band arising from the C=O stretching vibrations and N-H groups might form the hydrogen bonding; they are associated with protein conformation. Therefore, it is suitable as a probe to determine the different secondary structures of proteins and polypeptides (21,39).

In the present experimental work, the frequencies of the bond vibrations are easily determined by FTIR and the vibration spectra are directly related to the structural features of molecules. Rabbit's lens protein was greatly affected by exposure to intense green laser light from frequency doubled Nd:YAG (532 nm) (Figure 3). The decrease in the total soluble protein (Figure 1) and the change in the molecular weight of lens protein (Figure 2) are attributed to the conformational changes in protein secondary structure as noticed in FTIR spectra (Figure 6). Considerable changes in lens proteins might occur in which protein bonding changes and protein molecules clump together (40).

The lens is composed of water (65%) of two types, intracellular and extracellular. The intracellular water can be bound to the proteins as water of crystallization or be arranged in a layered structure. This intracellular environment for water is expected to slightly alter its vibration characteristics (41,42). Second-derivative FTIR spectral analysis was applied to locate the position of the overlapping components of the amide I and II bands and to assign them to different secondary structures (21,22,39). The obtained FTIR results (Figure 6), revealed a marked difference in the peak intensity ratio of amide I / amide II for the normal and treated lenses. The significant change in peak intensity ratio of amide I: amide II might be related to the different water contents in lenses. It has been reported that the cataractous lens contained less total water than normal lens (16,21). Furthermore, the peak intensity ratio of the amide I / amide II absorbance for the normal and treated lenses is assignable to unordered structures and was used to monitor the thermally induced structural transitions of the crystallin samples (43).

There are three common secondary structures in proteins, namely α -helix, β -turns and β -sheets. β -turns are conformations that enable protein to adopt globular structures, and their formation is often rate limiting for folding [44]. They are the smallest type of the secondary structure, joining other elements of secondary structures as α -helix and β -sheets, and abruptly change the direction of the polypeptide chain (45). The formed β -turn structure may serve as a nucleation site for folding/refolding of proteins (46).

β -sheets are another protein secondary structure conformation; although the importance of β -sheets in the folded structures of proteins has long been recognized and they are important for biological activities (47). Intermolecular β -sheet interactions

(bands $< 1620 \text{ cm}^{-1}$) are associated with bio-molecular recognition, protein quaternary structure, protein-protein interactions and peptide and protein aggregation, while intra-molecular β -sheet interactions (band between $1630\text{-}1620 \text{ cm}^{-1}$) are associated with protein folding (48).

Thus, vibrational spectra of the FTIR spectra, were directly related to the structural features of molecules, hence; our results indicate that the intermolecular β -sheets (bands $< 1620 \text{ cm}^{-1}$) transitionally exist after exposure to 532 nm for 6 and 18 seconds (Figure 4 and Figure 6). This radiation led to the formation of intra-molecular hydrogen-bonded β -sheet structure. The formation of such β -sheet structures resulted from the conversion of α -helix to β -sheet. On the other hand, increasing irradiation time to 18 sec resulted in insoluble and more folded lens protein, which reflects that the lens proteins become aggregated. As it has been suggested that protein insolubility depends on the content of β -sheet structure; the more β -sheet structure means the more insoluble protein (16).

In conclusion, the present study showed that intense green light from doubled frequency Nd:YAG laser in the nanosecond range seems to be harmless to the lens for both short term and prolonged exposure capable of inducing photo-thermal and photochemical damage. The obtained finding of FTIR provides information about the conformational changes in lens protein. These conformational changes may be responsible for the insolubility and aggregation of lens protein as indicated by protein concentration and SDS-PAGE. With the enormous expansion of laser use in medicine, industry and research, every facility must formulate and adhere to specific safety policies that appropriately address eye protection.

References

1. Shen Y R. The principles of nonlinear optics. John Wiley and Sons, Inc., Hoboken, New Jersey; 2002.
2. Agrawal G P. Applications of nonlinear fiber optics (4th ed.). Academic Press, San Diego, California, USA; 2006.
3. Boyd R W. Parametric versus nonparametric processes, In: Nonlinear Optics (3rd ed.), 2008. 13-15.
4. Han M, Giese G, Bille J. Second harmonic generation imaging of collagen fibrils in cornea and sclera. Opt express 2005; 13: 5791-7.
5. Brown DJ, Morishige N, Neekhra A, Minckler DS, Jester JV. Application of second harmonic imaging microscopy to assess structural changes in optic nerve head structure ex vivo. J Biomed Opt. 2007;12: 024029.

6. Galang J, Restelli A, Hagley EW, Clark C W. A green laser pointer hazard. *Natl Inst Stand Tech* 2010;1668: 1-9.
7. Te EA. The next generation in laser treatments and the role of the green light high-performance system laser. *Rev Urol* 2006; 8: S24–S30.
8. Walsh LJ. The current status of laser applications in dentistry. *Aust Dent J* 2003; 48:146–55.
9. Bloemendal H. Molecular and cellular biology of the eye lens. Wiley, New York; 1981. 1-47.
10. Wistow GJ, Piatigorsky J. Lens crystallins: the evolution and expression of proteins for a highly specialized tissue. *Annu Rev Biochem* 1988; 57: 479- 504.
11. Delaye M, Tardieu A. Short-range order of crystallin proteins accounts for eye lens transparency. *Nature* 1983; 302:415- 7.
12. Spector A. The search for a solution to senile cataracts. Proctor lecture. *Invest Ophthalmol Vis Sci* 1984; 25: 130-46.
13. Kalasinsky VF, Johnson FB, Ferwerda R. Fourier transform infrared and Raman microspectroscopy of materials in tissue. *Cell Mol Biol* 1998; 44: 141-4.
14. Boskey A. Mineral changes in osteopetrosis. *Crit Rev Eukaryo. Gene Expr* 2003;13: 109-16.
15. Petry R, Schmitt M, Popp J. Raman spectroscopy – a prospective tool in the life sciences. *Chem phys chem* 2003; 4: 14-30.
16. Lin SY, Li M J, Liang RC, Lee SM. Non-destructive analysis of the conformational changes in human lens lipid and protein structures of the immature cataracts associated with glaucoma. *Spectrochim Acta A Mol Biomol Spectrosc* 1998; 54: 1509 -17.
17. Lin SY, Chen K H, Li M J, Cheng W T and Wang S L. Evidence of octacalcium phosphate and type-B carbonated apatites deposited on the surface of explanted acrylic hydrogel intraocular lens. *J Biomed Mater Res B Appl Biomater.* 2004; 70: 203-8.
18. Lowry OH, Rosebrough NJ, Farr AL, Randall RJ. Protein measurements with Folin Phenol reagent. *J Biol Chem* 1951; 193: 265-75.
19. Laemmli UK. Cleavage of structural proteins during assembly of the head of bacteriophage T4. *Nature* 1970; 227: 680-5.
20. Lamba OP, Borchman D, Sinha SK, Shah J, Renugopalakrishnan V, Yappert MC. Estimation of the secondary structure and conformation of bovine lens crystallins by infrared spectroscopy: quantitative analysis and resolution by Fourier self-deconvolution and curve fit. *Biochem Biophys Acta.* 1993; 1163: 113- 23.
21. Haris PI, Chapman D. Analysis of polypeptide and protein structures using Fourier transform infrared spectroscopy. *Methods Mol Biol* 1994; 22: 183-202.
22. Jackson M, Mantsch HH. The use and misuse of FTIR spectroscopy in the determination of protein structure. *Crit Rev Biochem Mol Biol* 1995; 30: 95-120.
23. Snedecor GW, Cochran WG. *Statistical Methods*,» 6th ed., Ames., Iowa, USA;1976.
24. Rigas S, Morgello s, Goldman IS, Wong PT. Human colorectal cancers display abnormal Fourier-transform infrared spectra. *Proc Natl Acad Sci USA* 1990; 87: 8140-4.
25. Steinert RF, Puliafito CA. *Laser in ophthalmology: Principles and clinical applications of photodisruption.*, Philadelphia WB Saunders Co; 1985. 22- 35.
26. Puliafito CA, Wasson PJ, Steinert RF, Gragoudas ES. Neodymium –YAG laser surgery on experimental vitreous membranes. *Arch Ophthalmol* 1984;102: 843- 7.
27. Abdelkawi SA, Elawadi AI. Liquefaction of the vitreous humor floaters is a risk factor for lens opacity and retinal dysfunction. *J Am Sci* 2011; 7: 911-8.
28. Juhasz T, Loesel FH, Kurtz RM, Horvath C, Bille JF, Mourou G. Corneal refractive surgery with femtosecond lasers. *IEEE J Select Topics Quantum Electron* 1999; 5: 902–10.
29. Yilmaz S, Yilmaz E. Effect of melatonin and vitamin E on oxidative –antioxidative status in rats exposed to irradiation. *Toxicology* 2006; 222: 1-7.
30. Kessel L, Eskildsen L, Lundeman JH, Jensen OB, Larsen M. Optical effects of exposing intact human lenses to ultraviolet radiation and visible light. *BMC Ophthalmol* 2011; 11:41.
31. Regini JW, Grossmann JG, Timmins P, Harding JJ, Quantock AJ, Hodson SA. X-ray- and neutron-scattering studies of alpha-crystallin and evidence that the target protein sits in the fenestrations of the alpha crystallin shell. *Invest Ophthalmol Vis Sci* 2007;48: 2695-700.
32. Stradner A, Foffi G, Dorsaz N, Thurston G, Schurtenberger P. New insight into cataract formation: Enhanced stability through mutual attraction. *Phys Rev Lett* 2007; 99: 198103.
33. Takemoto L, Sorensen CM. Protein-protein interactions and lens transparency. *Exp Eye Res* 2008; 87: 496-501.
34. Dillon J, Roy D, Spector A, Walker ML, Hibbard LB, Borkman RF. UV laser photodamage to whole lenses. *Exp Eye Res* 1989; 49:959-66.
35. Davies MJ, Truscott RJ. Photo-oxidation of proteins and its role in cataractogenesis. *J Photochem Photobiol* 2001; 63:114-25.
36. Erckens RJ, Jongsma FH, Wicksted JP, Hendrikse F, March WF, Motamedi M. Raman spectroscopy in ophthalmology: from experimental tool to applications in vivo. *Lasers Med Sci* 2001;16: 236–52.
37. Chen KH, Cheng WT, LI M J, Yang DM, Lin SY. Calcification of senile cataractous lens determined by Fourier transform infrared (FTIR) and Raman microspectroscopies. *J Microsc* 2005; 219: 36–41.
38. Trevino SR, Schaefer S, Scholtz JM, Pace CN. Increasing protein conformational stability by optimizing beta-turn sequence. *J Mol Biol* 2007; 373: 211–8.
39. Susi H, Byler DM. Protein structure by Fourier transform infrared spectroscopy: second derivative spectra. *Biochem Biophys Res Commun* 1983; 115: 391-7.

40. Bron AJ, Vrensen GF, Koretz J, Maraini G, Harding JJ. The ageing lens. *Ophthalmologica* 2000; 214: 86-104.
41. Warwick R. *Anatomy of the Eye and Orbit*, Philadelphia, W. B. Saunders Co; 1976.
42. Kuck J FR Jr. Chemical constituents of the lens. In: Gray More CN. *Biochemistry of the Eye*. New York, Academic Press, Inc; 1970. 183-260.
43. Surewicz WK, Olesen PR. On the thermal stability of alpha-crystallin a new insight from infrared spectroscopy. *Biochemistry* 1995; 34: 9655-60.
44. Fullera AA, Du D, Liu F, Davoren JE, Bhabha G, Kroon G. Evaluating beta-turn mimics as beta-sheet folding nucleators. *Proc Natl Acad Sci USA* 2009;106:11067-72.
45. Rose GD, Young WB, Gierasch LM. Interior turns in globular proteins. *Nature* 1983; 304: 654-7.
46. Orpiszewski J, Schoromann N, Kluve-Beckerman M, Liepnieks JJ, Benson MD. Protein aging hypothesis of Alzheimer disease. *FASEB J* 2000; 14: 1255-63.
47. Khakshoor O, Nowick JS. Artificial beta-sheets: Chemical Models of beta-Sheets. *Curr Opin Chem Biol* 2008; 12:722-9.
48. Szalontai B. Membrane protein dynamics: Limited lipid control. *PMC Biophys* 2009; 2: 1-17.